

High-temperature heat capacity and thermal expansion of SrTiO₃ and SrZrO₃ perovskites

Dominique de Ligny and Pascal Richet

Laboratoire des Géomatériaux, URA CNRS 734, Institut de Physique du Globe de Paris 4, place Jussieu, 75252 Paris Cédex 05, France

(Received 17 March 1995)

The heat capacity and thermal expansion of SrZrO₃ and SrTiO₃ have been determined by drop calorimetry and energy-dispersive x-ray diffraction from 300 up to 1800 K or more. For both compounds, thermal history has a slight influence on relative enthalpies in the range 900–1400 K but a satisfactory precision was obtained through systematic quenches from 1820 K before the calorimetric measurements. Strontium titanate is cubic at room temperature. Up to 1800 K, its heat capacity increases smoothly and its thermal-expansion coefficient remains almost independent of temperature with a value of $3.23(2) \times 10^{-5} \text{ K}^{-1}$. At room temperature, strontium zirconate is orthorhombic (space group *Pbnm*). The phase transitions from orthorhombic *Pbnm* to orthorhombic *Cmcm* at 995 K and then to tetragonal *I4/mcm* at 1105 K are revealed by symmetric, λ -type variations of the heat capacity. A more diffuse thermal effect characterizes the *I4/mcm* to cubic *Pm3m* transition at 1440 K, above which the cubic phase shows an apparently low heat capacity at the highest temperatures. With the resolution of the x-ray technique, only the transition from orthorhombic *Pbnm* to orthorhombic *Cmcm* at 970 K was detected with a small volume change of 0.14%. Thermal expansion below 970 K is constant at $2.98(2) \times 10^{-5} \text{ K}^{-1}$. At higher temperatures, the apparent thermal expansion decreases smoothly from 2.78(2) to $2.43(2) \times 10^{-5} \text{ K}^{-1}$ between 1000 and 1800 K. With recent data on CaTiO₃, the effects of (Ca,Sr) and (Ti,Zr) substitutions on thermal expansion and on the energetics of the phase transitions are discussed.

INTRODUCTION

Compounds with a perovskite crystal structure have long been investigated especially in view of the ferroelectric properties that they commonly exhibit. More recently, the perovskite structure has attracted much interest because it is adopted by ceramic superconductors and also by the major mineral on earth, namely, (Mg,Fe)SiO₃ perovskites, which are stable at pressures higher than 250 kbar.¹

The actual CaTiO₃ perovskite mineral has an orthorhombic symmetry at room pressure and temperature. The aristotype of ABO₃ perovskites has a cubic symmetry, however, and the observed rhombohedral, orthorhombic or tetragonal symmetries result from tilting and distortion of the BO₆ octahedra.^{2,3} Orthorhombic perovskites frequently undergo a series of temperature-induced transitions to phases with a higher symmetry.^{4,5} Unfortunately, there are few reliable data pertaining to the energetics of these transitions because of the difficulties of precise calorimetric measurements at the generally high temperatures of these transitions. An exception is CaTiO₃, for which recent calorimetric measurement have shown two overlapping phase transitions at 1384 and 1520 K.⁶ The first one is narrow and shows a classical λ -type C_p variation, whereas the second one has an inverse λ -shape with a transition width of more than 400 K and a long tail at higher temperatures, indicative of considerable post-transition effects.

In this work, we have complemented the data on CaTiO₃ with new measurements on strontium titanate (SrTiO₃) and strontium zirconate (SrZrO₃) to investigate the influence of structure and (Ca,Sr) and (Ti,Zr) cation substitutions on the high-temperature thermodynamic properties of perovskites. At room pressure, strontium titanate transforms at 110 K from tetragonal to cubic. Up to its melting point, SrTiO₃ thus remains cubic (space group *Pm3m*) and will serve as a ref-

erence for the aristotype of ABO₃ perovskites. In contrast, strontium zirconate is orthorhombic at room temperature and undergoes a series of phase transitions which have been studied by thermal analysis and x-ray and neutron diffraction.⁷⁻⁹ At 970 K, SrZrO₃ changes from orthorhombic, *Pbnm*, to *Cmcm* symmetry, then at 1100 K to tetragonal *I4/mcm*, and eventually at 1440 K to the cubic aristotype *Pm3m*. Our primary goal was to determine the thermal effects of these transitions. We have complemented our calorimetric observations by x-ray-diffraction experiments up to 1800 K for SrZrO₃, and to 2000 K for SrTiO₃, i.e., at temperatures higher than in previous studies.

EXPERIMENTAL METHODS

Commercial samples (from Johnson-Matthey) with a purity better than 99% were investigated. According to the manufacturer, for SrTiO₃ the main impurities are Al₂O₃ (0.025 wt %), BaO (0.22), CaO (0.077), Na₂O (0.020), ZrO₂ (0.014). For SrZrO₃, they are Al₂O₃ (0.6 wt %), CaO (0.13), SiO₂ (0.47), BaO (0.33), Na₂O (0.01), and Fe₂O₃ (0.02). For both compounds, powder x-ray-diffraction patterns were similar for the starting products and for the materials recovered after the calorimetry measurements. In addition to the intended phases, they showed only one and two weak reflections ($I/I_{100} < 1\%$) of TiO₂ and ZrO₂ for SrTiO₃ and SrZrO₃, respectively. Cubic lattice parameters of $3.9051(8) \text{ \AA}$ for SrTiO₃ and $4.1029(9) \text{ \AA}$ for SrZrO₃ were obtained at room temperature from these patterns.

The two as-purchased perovskites had an initial grain size of about 1 μm . Observed by optical microscopy after 3-h heating at 1800 K in air in Pt cups, they presented a mosaic recrystallization texture associated with extensive sintering of μm - to mm-sized polycrystalline grains. For SrTiO₃, some crystals with an automorph octahedral habit had grown

up to a few tens of μm . As noted by Lytle,¹⁰ they appeared dark between crossed polarizers under a petrographic microscope. For SrZrO_3 , the sintered grains showed birefringent crystals of about $5 \mu\text{m}$ embedded in an optically isotropic matrix with a grain size of the order of $1 \mu\text{m}$. This contrasting birefringence is probably due only to grain size differences. For both perovskite samples, similar optical observations were made after subsequent thermal treatments at various temperatures.

Prior to the calorimetry measurements, the products were heated in air at temperatures between 1670 and 1870 K for about 15 min, quenched, ground, and reheated a few times to limit subsequent sintering in the calorimetry crucibles. After these heat treatments, the weight loss was about 0.5% and the initially white powders had become brownish and greenish-yellow in hue for SrTiO_3 and SrZrO_3 , respectively. About 6 and 9 g of SrTiO_3 and SrZrO_3 perovskites, respectively, were then loaded in a Pt-Rh 15% or Pt-Ir 15% crucible in the form of a coarse polycrystalline powder with a maximum grain size of a few hundred μm . The two 1-mm openings of the crucibles were rather tightly closed with creased platinum foils which prevented spilling of the powder during the drop in the calorimeter. There was no change in the mass of the samples during the series of calorimetric measurements. Likewise, no recrystallization of the coarse powders was observed at the end of the measurements.

Relative enthalpies $H_T - H_{273.15}$ (hereafter noted more simply $H_T - H_{273}$) were measured by drop calorimetry with the ice calorimeters and high-temperature setups already described in detail.^{11,12} Temperatures were measured to about 0.1 K with two thermocouples within the crucible itself, which ensured excellent precision and rapid detection of thermal stability. In general the heating stage of the experiments (in air) lasted less than an hour and complete cooling to 273 K after the drop (in argon) took about 20 min. The imprecision of the enthalpy measurements is about 0.05%. Measurements on $\alpha\text{-Al}_2\text{O}_3$, the calorimetric standard, indicate inaccuracies of less than 0.2% and 0.5% for the relative enthalpies and derived heat capacities, respectively, from 400 to 1800 K.¹¹

Heat capacities were determined by differentiation of least-squares fits made to the experimental relative enthalpies:

$$H_T - H_{273} = R_{T_0} + \int_{T_0}^T C_p dT, \quad (1)$$

where R_{T_0} is the relative enthalpy at a reference temperature T_0 (namely, 273 K for the low-temperature phase, or the lower transition temperature for high-temperature phases). For the heat capacity, we used empirical equations of the form

$$C_p = a + bT + c/T^2 + d/T^{0.5} + eT^2. \quad (2)$$

When available, adiabatic C_p data for temperatures higher than 273 K were included in the fits. To take into account the effects of phase transitions we incorporated into Eq. (2) expressions of the form

$$C_{pt} = A(1 - T/T_t)^\alpha, \quad \text{for } T < T_t \quad (3a)$$

or

$$C_{pt} = A(T/T_t - 1)^\alpha, \quad \text{for } T > T_t, \quad (3b)$$

where T_t is the transition temperature.

Thermal-expansion coefficients were determined from powder x-ray-diffraction experiments performed in an energy-dispersive configuration on the wiggler line of the DCI storage ring of Laboratoire d'Utilisation du Rayonnement Electromagnétique (Orsay). The high-temperature technique has been described previously.¹³ In brief, very finely powdered samples are loaded in the $400\text{-}\mu\text{m}$ hole drilled in a Pt 90%-Rh 10% heating wire, and the sample temperature is obtained from calibrations of the electrical power needed to heat the wire as a function of the melting points of a series of salts and silicates. The reported temperatures are accurate to within 10° . For the diffraction experiments, the x-ray beam was collimated to either 200×50 or $200 \times 30 \mu\text{m}^2$. The diffracted beam was analyzed with a Canberra planar germanium detector at 2θ angles of about 12° for energies comprised between 10 and 50 keV. The room-temperature diffraction patterns were used to determine the diffraction angle by comparison with reported Joint Committee for Powder Diffraction Standard data. In these experiments we thus measured only relative changes in cell parameters. Good quality patterns were recorded in about 7 and 5 min for SrTiO_3 and SrZrO_3 , respectively. On cooling after experiments at higher temperatures, the quality of the patterns was poor, owing to strong orientation effects resulting from extensive recrystallization. All measurements were thus made on heating. A number of very intense fluorescence lines of Sr, Zr, and Ti were observed in all the diffraction patterns. Fortunately, they were present at energies lower than those of the main diffraction peaks. For cell-parameter refinements, we used only reflections for which both the peak energy and linewidth could be determined reliably from 300 K up to the highest temperatures.

CALORIMETRY

General remarks

The experimental relative enthalpies are listed in Tables I and II where runs are labeled in chronological order. Along with previous measurements, they are also plotted in Figs. 1 and 2 in the form of mean heat capacities C_m :

$$C_m = (H_T - H_{273}) / (T - 273). \quad (4)$$

In this way experimental results can be examined without fitting bias that could affect heat capacities obtained from differentiation of relative enthalpies.

In a first series of measurements, we observed an anomalously high scatter in the relative enthalpies of both SrTiO_3 and SrZrO_3 . For SrTiO_3 , this lower reproducibility is particularly clear at around 800 K, especially after a number of measurements in the temperature range 800–1100 K (Fig. 1). For SrZrO_3 , it is between 900 and 1400 K, and especially between 1130 and 1300 K, that the scatter appears when the data are plotted at a greater scale (Fig. 3). These features indicate that some structural changes took place in an irreproducible way during cooling of the materials in the calorimeter. As a result, the final state of the sample differed slightly from one experiment to another, introducing some bias in determinations of heat capacities from the enthalpies measured in the first series.

To limit thermal history effects in a second series of experiments, before each measurement the samples were

TABLE I. Relative enthalpy of the SrTiO₃ perovskite (kJ/mol).

No.	T (K)	$H_T - H_{273}$	No.	T (K)	$H_T - H_{273}$
First series (no heat treatment)			Second series (after a quench from 1820 K)		
EZ1	562.5	31.130	EZ36	405.2	13.285
EZ17	581.2	33.796	EZ33	489.6	22.979
EZ8	638.4	40.254	EZ35	544.7	29.203
EZ20	671.4	44.227	EZ31	594.8	35.045
EZ22	684.7	45.764	EZ22	645.3	41.035
EZ10	728.5	51.030	EZ32	682.9	45.475
EZ15	763.0	55.427	EZ43	718.8	49.645
EZ18	794.1	59.143	EZ26	737.1	51.786
EZ6	835.7	63.191	EZ44	747.6	52.850
EZ14	865.1	67.547	EZ45	752.0	53.866
EZ9	881.7	69.070	EZ30	760.9	54.888
EZ19	899.0	71.500	EZ29	772.7	56.468
EZ7	902.4	71.684	EZ28	807.6	60.539
EZ16	943.0	77.267	EZ25	884.8	69.907
EZ4	999.6	83.411	EZ27	973.5	80.882
EZ21	1087.4	95.146	EZ24	1075.8	93.714
EZ5	1133.6	100.53	EZ40	1170.6	105.70
EZ11	1278.0	119.16	EZ37	1199.7	109.36
EZ12	1462.9	142.83	EZ38	1348.8	128.31
			EZ39	1505.8	148.91
			EZ41	1652.0	168.36
			EZ42	1804.0	187.81

heated at 1820 K for 10 min in air in an electric muffle furnace and then quenched by dipping the crucible in water. Experience showed that this quenching procedure ensured an acceptable reproducibility for both perovskites, albeit not as good as the 0.05% obtained with our calorimetric setup for well-behaved materials. Comparisons of these results with those of the first series indicate that the anomalous results are the lowest ones, which could be up to 1% too low. Among the anomalous results, the points plotted in Fig. 3 as open circles indicate runs for which thermal equilibration to 273 K in the calorimeter was twice as long as usual, suggest-

ing that the endothermic process responsible for the low enthalpies was favored by a slower cooling rate when the thermal contact between the crucible and the heat receiver of the ice calorimeter was not so good.

Strontium titanate

The results of Table I generally agree with the previous drop-calorimetry data of Coughlin and Orr¹⁴ which are on the average 0.4% lower than ours (Fig. 1) and have a precision similar to that of our study. Exceptions are above 1500 K, where the results of Coughlin and Orr¹⁴ are 0.8%–1.0%

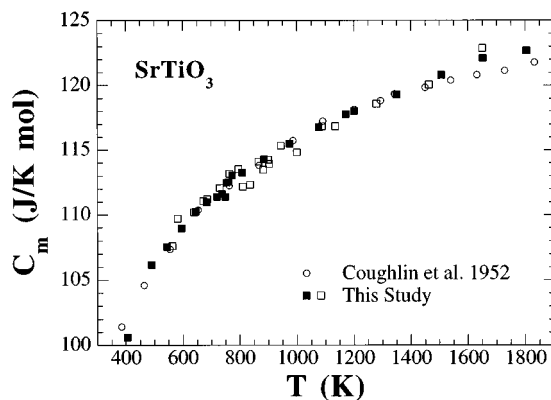


FIG. 1. Mean heat capacity of the SrTiO₃ perovskite. The open and solid squares refer to the first and second series of experiments, respectively. The results of Coughlin and Orr (Ref. 14) have been referred to 273 K with the C_p equation of Table III.

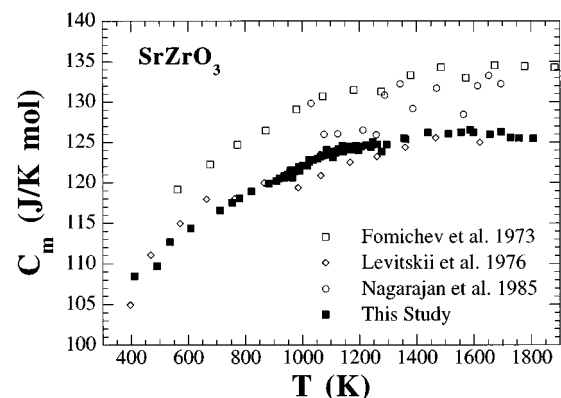


FIG. 2. Mean heat capacity of the SrZrO₃ perovskite. All the $H_T - H_{298}$ data have been referred to 273 K with the C_p equation of Table III.

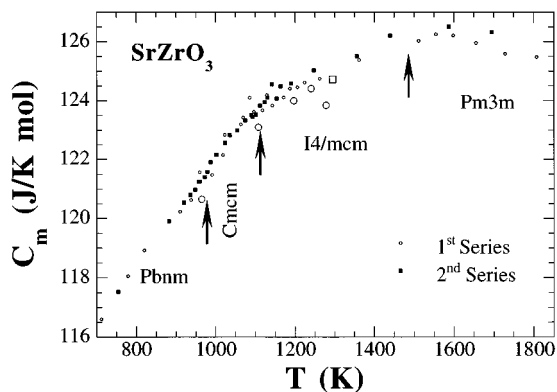


FIG. 3. Mean heat capacity of the SrZrO_3 perovskite in the transition regions. The open circles and square indicate the experiments with an unusually slow cooling rate in the first and second series of measurements, respectively, which were discarded in C_p fits. The arrows indicate the transition temperatures as determined by Carlsson (Ref. 7) from DTA and x-ray-diffraction experiments.

lower than ours. As discussed previously,⁶ similar systematic differences between both laboratories have been found for CaTiO_3 in the same temperature interval. At lower temperatures, good agreement is also found with the adiabatic measurements of Todd and Lorensen¹⁵ which have been used in conjunction with our results to derive the heat-capacity equation listed in Table III.

Strontium zirconate

As shown in Fig. 2, previously published relative enthalpies for SrZrO_3 span an extremely wide range of values. Our data agree reasonably well with the drop-calorimetry measurements of Levitskii, Tsagareishvili, and Gvelesiani,¹⁶ and they also join smoothly with the adiabatic measurements made by King and Weller¹⁷ from 50 K to room temperature. In contrast, there is poor agreement with the other drop-calorimetry results of Fomichev *et al.*,¹⁸ selected in a recent compilation,¹⁹ which are systematically about 7% higher than ours and join less well with the low-temperature data.¹⁷ If the reason for these discrepancies is unknown, their sheer magnitude does not seem reconcilable with sample differences. Important differences are also found with the heat-flow measurements of Nagarajan *et al.*²⁰ As apparent in Fig. 2, they are likely not significant in view of the low precision of these data.

Looking in more detail at the results, one observes two slight inflexions at around 1000 and 1100 K in the mean heat-capacity curves. These inflexions are clearly better defined in the second series of measurements than in the first one (Fig. 3). As an objective way of determining heat capacities below 1400 K, we have made spline fits to the results of the second series, excluding only the measurements with unusually long cooling times in the calorimeter. These heat capacities obtained by differentiation of the spline functions show two symmetric λ -type transitions with a maximum at 995 and 1105 K (Fig. 4). The coefficients of the analytical expressions (2) and (3) fitted to the relative enthalpies are given in Table III. As apparent in Fig. 4, they give heat capacities in good agreement with those of spline fits. At the

highest temperatures, the spline fit points to a C_p decrease which would delineate an additional, smeared out peak at around 1450 K (Fig. 4). Actually, this decrease is also found in the fits made with Eqs. (1) and (2) to the consistent experimental data of both series.

Estimation of the enthalpy and entropy effects of these transitions is made difficult by the arbitrariness of the baseline over which the λ -type anomalies are to be integrated. The baseline plotted in Fig. 4 is the heat capacity given by the combination of Debye and Einstein temperatures reported by King and Weller,¹⁷ to which we have added the $C_p - C_v$ difference calculated from the thermal-expansion coefficient reported in the next section (below 970 K) and a bulk modulus of 1500 kbar estimated from those of related perovskites.²¹ With this baseline, the enthalpies and entropies of transition are 1.5 ± 0.1 kJ/mol and 1.7 ± 0.3 J/mol K for the 995 K transition, and 0.5 ± 0.1 kJ/mol and 0.45 ± 0.3 J/mol K for the 1105 K transition.

X-RAY DIFFRACTION

Strontium titanate

All the reflections observed for SrTiO_3 are consistent with the accepted cubic cell. The unit-cell parameter and volume were determined from the seven reflections that could be followed from room to the highest temperatures. The results are listed in Table IV and plotted in Fig. 5. A constant value of $\alpha = 3.23(2) \cdot 10^{-5} \text{ K}^{-1}$ accounts for all our measurements over a temperature interval of more than 1500 K. Below room temperature, available data do point to a decrease of α down to the temperature of the cubic-tetragonal transition (Table V). This trend is also borne out by the data of Devanarayanan and Narayanan,²³ obtained on a single crystal with a Fizeau interferometer, which shows an increase of α from $2.2(3) \cdot 10^{-5} \text{ K}^{-1}$ at 290 K to an average value of about $3.3 \cdot 10^{-5} \text{ K}^{-1}$ above room temperature.

Strontium zirconate

For a slightly distorted perovskite like SrZrO_3 , most of the reflections characteristic of an orthorhombic symmetry can be clearly observed at small interplanar distances, i.e., in the high-energy end of our patterns where the diffracted intensity is rapidly declining. Hence, we could index only on the basis of a pseudocubic cell, double of the ideal cubic one, the main reflections present in the energy-dispersive x-ray-diffraction patterns. The unit-cell volumes obtained from the five best quality reflections followed up to 1800 K are listed in Table IV and plotted in Fig. 6. They show good agreement with literature data, except in the upper range of previous measurements, where they give somewhat smaller volumes, especially with respect to the x-ray diffraction made by Zhao and Weidner²⁵ up to 1470 K on samples heated on a platinum strip.

A close inspection of our results show a slight kink at around 970 K in the volume-temperature relationship. The volume change of 0.14% is close to the precision limit of our measurements, but it seems unlikely that the good correspondence between the temperature of this kink and that of the first phase transition observed near 995 K in calorimetry is fortuitous. Up to 970 K, we find a constant thermal expansion

TABLE II. Relative enthalpy of the SrZrO₃ perovskite (kJ/mol).

No.	T (K)	$H_T - H_{273}$	No.	T (K)	$H_T - H_{273}$
	First series (no heat treatment)			Second series (after a quench from 1820 K)	
EW13	411.0	14.954	EW53	486.9	23.792
EW12	535.0	29.501	EW88	754.0	56.510
EW16	608.3	38.354	EW54	881.9	72.991
EW11	711.6	51.124	EW67	919.3	77.883
EW18	778.3	59.637	EW64	935.5	80.009
EW8	819.7	64.997	EW62	947.8	81.617
EW17	909.5	76.509	EW52	956.1	82.800
EW37	937.4	80.127	EW55	959.3	83.195
EW7	959.0	83.379	EW60	972.2	84.864
EW36sc	964.0	83.352	EW68	978.7	85.782
EW19	990.1	87.092	EW66	986.9	87.008
EW20	1017.9	90.975	EW69	1001.1	88.923
EW45	1022.1	91.997	EW65	1023.3	91.937
EW28	1036.3	93.720	EW51	1034.7	93.541
EW23	1062.7	97.270	EW58	1053.9	96.021
EW27	1069.0	98.230	EW63	1074.0	98.768
EW1	1085.1	100.76	EW79	1089.8	100.86
EW34	1095.8	101.70	EW57	1092.7	101.17
EW30sc	1107.3	102.68	EW61	1101.1	102.27
EW33	1117.1	104.38	EW75	1110.9	103.74
EW6	1128.3	106.20	EW73	1122.8	105.32
EW38	1142.3	107.63	EW78	1130.4	106.39
EW21	1170.5	111.37	EW71	1140.7	108.06
EW49	1186.5	113.63	EW80	1153.1	109.17
EW26sc	1195.9	114.42	EW77	1163.5	110.84
EW41	1205.9	116.09	EW72	1189.1	114.11
EW2	1223.6	118.44	EW74	1247.3	121.80
EW43sc	1239.9	120.27	EW81sc	1294.5	127.38
EW35	1261.1	123.24	EW83	1356.1	135.92
EW44sc	1277.5	124.38	EW82	1439.5	147.20
EW3	1361.1	136.41	EW84	1586.9	166.21
EW4	1510.8	155.98	EW87	1694.7	179.57
EW46	1554.8	161.81			
EW48	1597.8	167.19			
EW5	1655.5	174.12			
EW50	1727.9	182.71			
EW9	1806.6	192.42			

sion $\alpha = 2.98(2) \cdot 10^{-5} \text{ K}^{-1}$. Above 970 K none of the other phase transitions observed in calorimetry have a clear signature in the unit-cell volumes. One simply observes that the thermal-expansion coefficient decreases slightly with temperature as given by

$$\alpha = 3.20 \cdot 10^{-5} - 4.29 \cdot 10^{-9} T \text{ (K}^{-1}\text{)}. \quad (5)$$

With this equation, α decreases linearly from $2.78(2) \cdot 10^{-5} \text{ K}^{-1}$ at 970 K to $2.43(2) \cdot 10^{-5} \text{ K}^{-1}$ at 1800 K when neglecting possible volume changes across the transitions. In fact, three low-intensity reflections inconsistent with a pseudocubic cell were observed between 23 and 26 keV, corresponding to the 311, 320, and 321 reflections of the pseudocubic double cell (Fig. 7). Their position could not be determined

with the precision required for calculations of orthorhombic cell parameters. Qualitatively, however, their disappearance at higher temperatures constrain the nature of the phase transitions. The 320 and 321 reflections are consistent with the two orthorhombic space groups proposed by Ahtee, Glazer, and Hewa,⁹ but are forbidden in the tetragonal symmetry. They are no longer clearly visible in patterns recorded at temperatures higher than 710 and 1000 K, respectively, which indicates that the sample had still an orthorhombic symmetry at 1000 K. The 311 reflection is forbidden in the cubic symmetry. It becomes very weak above 1200 K and the decrease of its intensity shown in Fig. 8 is indeed consistent with a transition to the cubic form at 1440 K as reported by Carlsson.⁷

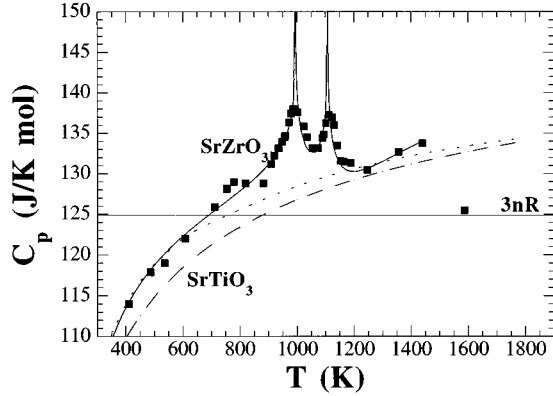


FIG. 4. High-temperature heat capacity of the SrZrO₃ perovskite as determined from spline fits to the data of the second series of experiments (solid squares) with a fitting parameter of 0.65%. The solid line represents the heat capacities given by the equations of Table III and the dotted curve the baseline lattice heat capacity (see text). For comparison, we have included the heat capacity of SrTiO₃ as the dashed curve and the Dulong and Petit limit as the horizontal line.

DISCUSSION

Structural changes on cooling of perovskites

An important difficulty encountered in this drop-calorimetry study is the influence of thermal history on the measured relative enthalpies of both SrTiO₃ and SrZrO₃ perovskites. As a matter of fact, the biggest effect below 1500 K is of the order of 1 kJ/mol only, and the current precision of solution calorimetry experiments on perovskites (i.e., 1–3 kJ/mol) (Ref. 27) is probably insufficient to determine such enthalpy differences between samples with different thermal histories. Although this slight influence could be observed only thanks to the intrinsically good precision of our measurements, for annealed samples it hampers heat-capacity de-

TABLE IV. Relative changes in unit-cell volumes of SrTiO₃ and SrZrO₃ perovskites.^a

<i>T</i> (K)	<i>V/V</i> ₀	<i>T</i> (K)	<i>V/V</i> ₀
	SrTiO ₃		SrZrO ₃
300	1.0000	300	1.0000
435	1.0042	405	1.0029
530	1.0070	490	1.0054
630	1.0103	605	1.0088
720	1.0130	710	1.0125
785	1.0154	820	1.0156
865	1.0185	900	1.0183
1000	1.0234	970	1.0213
1080	1.0260	1000	1.0227
1155	1.0278	1040	1.0237
1235	1.0303	1080	1.0247
1345	1.0334	1120	1.0260
1460	1.0380	1155	1.0264
1560	1.0419	1195	1.0277
1710	1.0451	1235	1.0287
1830	1.0526	1270	1.0301
		1310	1.0310
		1350	1.0320
		1385	1.0330
		1480	1.0357
		1585	1.0387
		1700	1.0410
		1800	1.0441

^aWith respect to the room-temperature volumes of 59.55 (1) and 69.06 (6) Å³ determined independently for SrTiO₃ and SrZrO₃, respectively.

terminations and blurs the calorimetric effects of the phase transitions of SrZrO₃. In particular, spline fits made to the first series of experiments yield much broader and less intense *C_p* peaks than shown in Fig. 4 for samples systemati-

TABLE III. Coefficients of heat capacity and enthalpy equations, $C_p = A|(1 - T/T_i)|^\alpha + a + bT + c/T^2 + d/T^{1/2}$ (J/mol K), with $H_T - H_{273}$ as given by Eqs. (2) and (3).

ΔT (K) ^a	<i>A</i>	α	<i>T_i</i>	<i>a</i>	10 ³ <i>b</i>	10 ⁻⁵ <i>c</i>	<i>d</i>	<i>T</i> ₀	<i>R</i> ₇₀	AAD(%)
SrTiO ₃										
270–1800				134.581	4.5567	-11.979	-414.3	273		0.12 ^b
SrZrO ₃										
270–995	63.717	-0.0365	995	55.945	8.7668	-17.344		273		0.08 ^c
995–1105	-812.192	0.0043	1105					995	88 080	
	922.568	-0.00443	995							0.05
1105–1440	80.037	-0.0553	1105	71.167		-469.085		1105	102 920	0.09
1440–1800				76.638		1250.18		1440	147 203	0.12
Baseline				134.366	3.8632	-13.209	-272.66	273		0.05

^a ΔT is the temperature range of validity of the equations; AAD is the average absolute deviation of the fitted values from the experimental data.

^bAAD of 0.12% for the adiabatic *C_p* data of Todd and Lorenson (Ref. 15) and 0.37% for the relative enthalpy measurements of Coughlin and Orr (Ref. 14).

^cAAD of 0.12% for the adiabatic *C_p* data of King and Weller (Ref. 17) and 1.38% for the relative enthalpy measurements of Levitskii, Tsagareishvili, and Gvelesiani (Ref. 16).

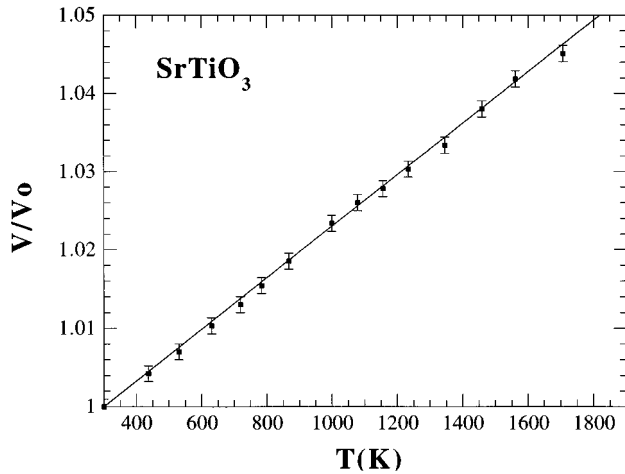


FIG. 5. Relative changes of the unit-cell volumes of the SrTiO_3 perovskite.

cally heated at 1820 K and then quenched prior to the measurements.

As noted above, the anomalous calorimetric results are the lowest ones, which might suggest that some exothermic structural changes took place less extensively on cooling for the samples annealed as a result of previous experiments (in the first series) than for the quenched samples (of the second series). Given the rapid time scale and constant oxygen fugacity conditions of our experiments, recovery of dislocations or point defects like oxygen vacancies seems unlikely major effects. Alternatively, too low enthalpies could result from endothermic changes developing more on cooling in annealed than in quenched samples. In the extensive literature devoted to SrTiO_3 , one actually finds that thermal history has significant effects on the thermodynamic properties and phase transition at low temperatures. The most extensive investigation, by Hatta *et al.*,²⁸ dealt with either polydomain

TABLE V. Thermal-expansion coefficients of SrTiO_3 and SrZrO_3 perovskites (10^{-5} K^{-1}).

α	ΔT (K)	Ref.
SrTiO_3		
2.82	110–300	Lytle (Ref. 10)
2.59	110–300	Itoh <i>et al.</i> (Ref. 22)
2.16	290	Devanarayanan and Narayanan (Ref. 23)
3.36	470	
3.12	570	
3.23 (2)	300–2000	This study
SrZrO_3		
2.63	298–590	Branson (Ref. 24)
2.80	590–970	
2.98 (17)	273–970	Zhao and Weidner (Ref. 25)
3.24 (33)	970–1100	
3.75 (22)	1100–1440	
2.65 (3)	298–1675	Mathews, Mirza, and Momin (Ref. 26)
2.98 (2)	300–995	This study
2.61 (10)	995–1800	This study (average value)

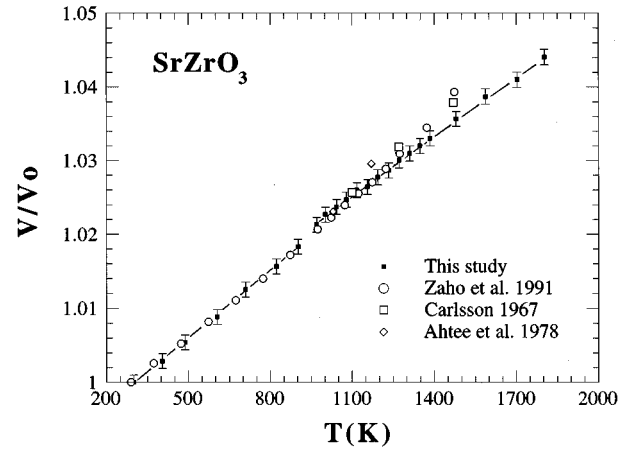


FIG. 6. Relative changes of the unit-cell volumes of the SrZrO_3 perovskite.

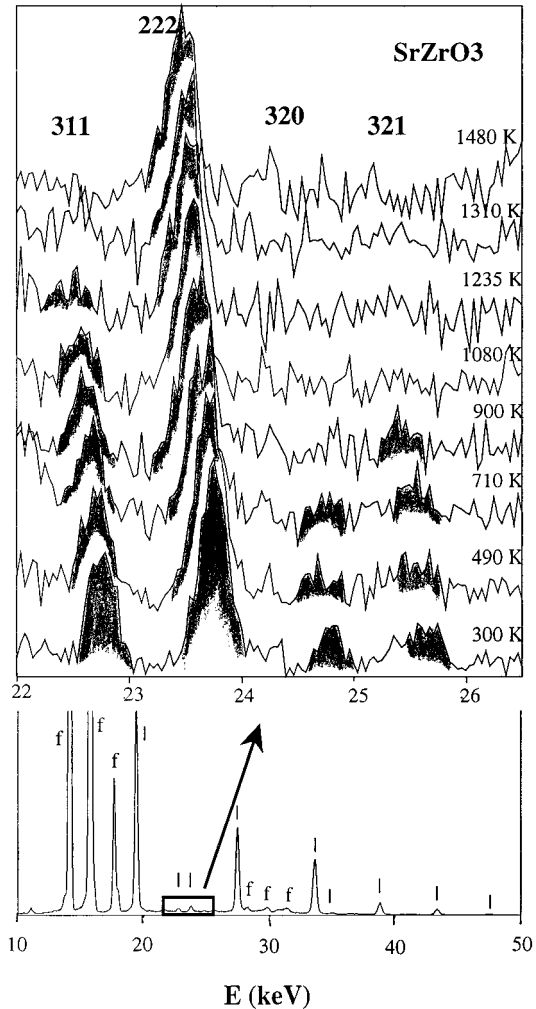


FIG. 7. Phase transitions of SrZrO_3 perovskite as evidenced by the changes in the intensity of the 311, 320, and 321 reflections of the pseudocubic double cell in the energy-dispersive x-ray-diffraction patterns. For comparison, the entire pattern recorded at 300 K is included at the bottom, where the fluorescence peaks of Sr and Zr are indicated by *f*, and the actual reflections by *l*.

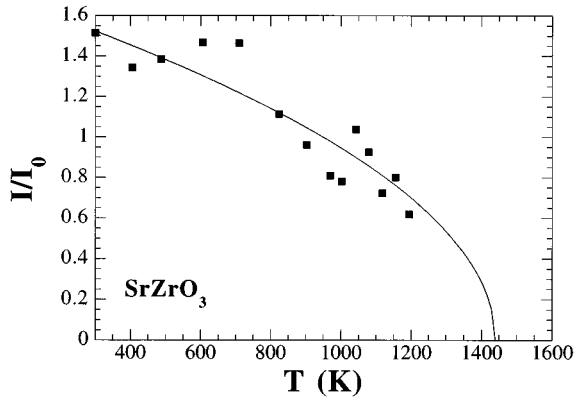


FIG. 8. Relative intensity of the 311 reflection of the SrZrO₃ perovskite with respect to the main reflection. The hand drawn curve shows the consistency of these intensities with the transition to a cubic phase reported at 1440 K (Ref. 7).

samples (slowly cooled after a long annealing at 1620 K) or monodomain samples (stabilized by thermal strain through a quench after their Verneuil synthesis near 2100 K). The quenched samples showed a higher heat capacity and a much sharper cubic to tetragonal transition at 110 K than annealed samples. Hatta *et al.*²⁸ related the C_p difference to the mobility of the boundaries of partially formed domains, even in almost monodomain samples, whereas the phase transition was smeared out in annealed SrTiO₃ samples because of inhomogeneities of thermal strain. The qualitative similarity of these features with our observations at higher temperatures suggests that this interpretation could also account for much of the influence of thermal history on the heat capacity of SrZrO₃. For SrTiO₃, however, the range of our measurements is much higher than the cubic to tetragonal transition temperature. This precludes interpreting the influence of thermal history in terms of formation and mobility of shape and stress-dependent domains, and could point instead to an unusually high influence of thermal strain on the heat capacity, which remains to be investigated in more detail.

Phase transitions of strontium zirconate

Because of the slight distortion of SrZrO₃, it has been argued that impurities, minor departures from nominal stoichiometry, or changes in synthesis temperatures could result in different crystal symmetries and phase transitions. From x-ray-diffraction experiments, van Roosmalen, van Vlanderen, and Cordfunke²⁹ recently reported a cubic symmetry (space group $P2_13$, with a double perovskite cell) for samples prepared below 1520 K, transforming at 1020 ± 30 K and 1273 ± 30 K into space groups $P2/n\bar{3}$ and $Pm\bar{3}m$, respectively, without calorimetric effects in differential scanning calorimetry measurements. We did not try to check this sequence of transitions because of the high temperatures aimed at in our study. We just note that our calorimetry and x-ray-diffraction results are consistent with previous structural data obtained for samples prepared at higher temperatures. The heat-capacity peaks apparent at 995 ± 5 , 1105 ± 5 , and 1440 ± 25 K (Fig. 4) correspond well to the three phase transitions at 1000 ± 25 , 1130 ± 25 , and 1430 ± 25 K originally reported by Carlsson⁷ from differential thermal analysis

(DTA). From x-ray diffraction Carlsson⁷ interpreted these changes in terms of transitions from orthorhombic to cubic symmetry through two different tetragonal phases. From neutron-diffraction experiments made at 1030 and 1170 K Ahtee, Glazer, and Hewat⁹ actually assigned the first of these transitions as a change from orthorhombic, $Pbnm$, to $Cmcm$ symmetry, and confirmed that the second transition was leading to tetragonal $I4/mcm$ symmetry.

From cell-parameter refinements, Zhao and Weidner²⁵ concluded that the phase transitions of SrZrO₃ are first order, albeit “nearly continuous and very close to the second order.” As previously observed for CaTiO₃,⁶ the enthalpy of SrZrO₃ is more sensitive than the volume to phase transitions. For both perovskites, the calorimetric effects points instead to λ -type transitions, which are in fact much sharper than the λ -type tetragonal to cubic transition of SrTiO₃. For SrZrO₃, the main feature of these transitions is their great width and almost symmetrical shape. The critical exponents of the heat-capacity equations are listed in Table III, but they do not warrant any comments because they have been obtained by derivation of indirect enthalpy measurements which do not extend up to the immediate vicinity of transitions. Unfortunately, none of the available x-ray-diffraction studies^{7,9,25} has also the accuracy required to evaluate critical exponents of the small spontaneous strain. In fact, the example of the tetragonal to cubic transition of SrTiO₃ suggests that such determinations could be made difficult in the vicinity of the transition temperature by the existence of domains and slight negative deviations of lattice parameters from critical behavior.^{30,31}

Phenomenologically, the symmetric nature of the calorimetric λ -type anomalies implies that the transitions cannot be understood in terms of mean-field theory, which does not predict any post-transition effects. The order parameter usually associated with phase transitions of perovskites is the tilting angle ϕ about the threefold $(111)_p$ axis of the regular BO_6 octahedra [calculated as $\phi = \cos^{-1}(\sqrt{2}a^2/bc)$, where a , b , and c are the $Pbnm$ unit-cell parameters].³² For SrZrO₃ at room temperature, this angle is 4° . Even though the variation with temperature of ϕ is loosely constrained by x-ray-diffraction data, it appears that this single order parameter cannot account for the transitions because of their symmetric width. Broad transitions for ferroelectric perovskites have been associated with an order-disorder component and a decoupling of the soft-mode behavior with the observed global transition.^{33,34} This suggests that different order parameters are needed to account for spontaneous strain, order disorder, and the cooperative component of the transition (which could include the effects of strongly interacting defects that are often associated with broad transitions).

Concerning the last transition to the cubic form near 1440 K, the steady decrease with temperature of the heat capacity at the highest temperatures warrants some comments. For CaTiO₃, the heat capacity of the cubic phase also decreases continuously,⁶ in a temperature range where a high ionic conduction due to oxygen mobility has been reported.³⁵ In contrast to that of CaTiO₃, the heat capacity of SrZrO₃ becomes apparently lower than the baseline defined by measurements at lower temperatures. It even decreases further to values much lower than the Dulong-Petit limit of 125 J/mol K. The actual enthalpy of SrZrO₃ is too low by about 8

kJ/mol at 1800 K with respect to a "normal" behavior. Transposed drop calorimetry experiments could thus determine whether the low heat capacity of the cubic phase is spurious or not. If spurious, this decrease would result from structural changes during quenches of the cubic phase. In this case, H_{273} would have to increase systematically and smoothly with the quench temperature to account for the correct precision of both series of measurements. Accepting this unlikely dependence, two puzzling questions would remain. Why would the heat capacity then be correct just above the transition temperature? And how could quenches performed from an approximately constant temperature of 1820 K, prior to the runs of the second series, have ensured a good precision at lower temperatures? In fact, a similarly low heat capacity of 74 J/mol K is indicated by measurements on ZrO_2 above 1500 K,³⁶ once the transition from monoclinic to tetragonal symmetry has been passed. Hence, there is no simple explanation for these apparently low heat capacities.

Phase transitions and distortion of perovskites

The distortion of ABO_3 perovskites is commonly described in terms of simple parameters such as the aforementioned tilting angle ϕ or the tolerance factor $t = \langle A-O \rangle / \sqrt{2} \langle B-O \rangle$ (where $\langle A-O \rangle$ and $\langle B-O \rangle$ are the average interatomic distances). The use of ϕ is restricted to the centrosymmetric perovskites when the BO_6 octahedra is considered as rigid. Ideal, cubic perovskites would have a tolerance factor unity and a tilting angle zero. At around 50 K, the tilting angle of $SrTiO_3$ is 1.5° (Ref. 11) and this angle vanishes at 110 K at the tetragonal to cubic transition. When replacing Ti by Zr at room temperature, the increase of BO distances would result in too big SrO_8 dodecahedra in a cubic unit cell and this polyhedra mismatch leads to an orthorhombic symmetry through tilting of the BO_6 octahedra with an angle ϕ of 6° .⁸ Likewise, substitution of Sr by Ca leads to an angle ϕ of 10° for $CaTiO_3$.³⁷

The structure of these compounds can be viewed as a network of corner-linked rigid octahedra. It has been suggested that the effects of the B and A cations on thermal expansion of ABO_3 perovskites result from dilation of the rigid octahedra and decrease of the tilting angle with increasing temperature, respectively.^{38,25} Because the tilting angle decreases through the successive phase transitions, its variations eventually no longer contribute to thermal expansion, whence the general decrease of α of $SrZrO_3$ from 2.98 to $2.43 \cdot 10^{-5} \text{ K}^{-1}$ between 300 and 1800 K. If thermal expansion were mainly due to the dilation of the rigid octahedra in

the cubic form, it should be similar for ABO_3 perovskites with the same B cation regardless of the A cation. For instance, the thermal-expansion coefficient of $SrZrO_3$ should tend toward that of the $BaZrO_3$ perovskite, which is already cubic at room temperature. The thermal-expansion coefficient of $BaZrO_3$ [$2.06 \cdot 10^{-5} \text{ K}^{-1}$ at 870 K (Ref. 25)] is in fact somewhat smaller than that of the cubic form of $SrZrO_3$. Likewise, the thermal-expansion coefficients of $CaTiO_3$ and $SrTiO_3$ at 1400 K are $3.87 \cdot 10^{-5} \text{ K}^{-1}$ ³⁷ and $3.23 \cdot 10^{-5} \text{ K}^{-1}$, respectively, which also indicates that the influence of the A cation on thermal expansion is not negligible, contrary to the simple model described above.^{38,25}

Turning finally to the systematics of the energetics of the phase transitions in ABO_3 perovskites, one remarks an obvious relationship between the overall enthalpies and entropies of transition and the magnitude of the initial tilting angle of the low-temperature phase. For $CaTiO_3$ this enthalpy associated with the vanishing of the 10° distortion is 6500 J/mol at around 1500 K,⁶ whereas it is 2000 J/mol at around 1000 K for the initial 6° tilting angle of $SrZrO_3$ and 20 J/mol (Ref. 28) at 110 K for the 1.5° angle of $SrTiO_3$. No clear thermal effect has been shown for $CaGeO_3$ at around 500 K (Ref. 39) with an angle of 4° , but the precision of the measurements does not rule out total enthalpy effects of a few hundred joules. For a $A^{2+}B^{4+}O_3$ centrosymmetric perovskite this trend is qualitative only because, as noted above, the use of the single order parameter ϕ cannot account for all the transition effects. Quantitative correlations would require accurate crystal structure refinement through the transition for determinations of the thermal expansion associated with the tilting angle. In any case, the tilting angle as an order parameter does not consider atomic bonding. Hence, the trend between the tilting angle and the energetics of the transitions cannot be used for other perovskites, like $NaMgF_3$, for which vanishing of the 15° tilting angle is associated with an overall enthalpy effect of 1500 J/mol at around 1050 K.^{40,41} As compared with the above data for $A^{2+}B^{4+}O_3$ perovskites, this small value results, of course, from weaker atomic bonding.

ACKNOWLEDGMENTS

We thank D. Andrault, F. Guyot, and J. P. Poirier for their constant interest in the high-temperature properties of perovskites, C. Téqui and A. Bouhifd for their help with the calorimetric measurements, P. Bazboux for fruitful discussions, and D. Andrault for a careful reading of the paper. Contributions from IPGP and CNRS-INSU-DBT are also acknowledged.

¹ *Perovskite: a Structure of Great Interest to Geophysics and Material Science*, AGU monograph, Vol. 45, edited by A. Navrotsky and D. J. Weidner (American Geophysical Union, Washington, D.C., 1989).

² A. M. Glazer, *Acta Crystallogr. B* **28**, 3384 (1972).

³ A. M. Glazer, *Acta Crystallogr. A* **31**, 756 (1975).

⁴ K. S. Aleksandrov, *Ferroelectrics* **16**, 801 (1976).

⁵ K. S. Aleksandrov, *Ferroelectrics* **20**, 61 (1978).

⁶ F. Guyot, P. Richet, Ph. Courtial, and Ph. Gillet, *Phys. Chem. Minerals* **20**, 141 (1993).

⁷ L. Carlsson, *Acta Crystallogr.* **23**, 901 (1967).

⁸ A. Ahtee, M. Ahtee, A. M. Glazer, and A. W. Hewat, *Acta Crystallogr. B* **32**, 3243 (1976).

⁹ A. Ahtee, A. M. Glazer, and A. W. Hewat, *Acta Crystallogr. B* **34**, 752 (1978).

¹⁰ F. Lytle, *J. Appl. Phys.* **35**, 2212 (1964).

- ¹¹P. Richet, Y. Bottinga, L. Denielou, J. P. Petitet, and C. Téquie, *Geochim. Cosmochim. Acta* **46**, 2639 (1982).
- ¹²P. Richet, P. Gillet and G. Fiquet, in *Thermodynamic Data: Systematics and Estimation*, edited by S. Saxena (Springer-Verlag, New York, 1992), p. 97.
- ¹³P. Richet, P. Gillet, A. Pierre, A. Bouhifd, I. Daniel, and G. Fiquet, *J. Appl. Phys.* **74**(9), 5451 (1993).
- ¹⁴J. P. Coughlin and R. L. Orr, *J. Amer. Chem. Soc.* **75**, 530 (1953).
- ¹⁵S. S. Todd and R. E. Lorenson, *J. Amer. Chem. Soc.* **74**, 2043 (1952).
- ¹⁶V. A. Levitskii, D. Sh. Tsagareishvili, and G. G. Gvelesiani, *Teplofiz. Vys. Temp.* **14**, 78 (1976).
- ¹⁷E. G. King and W. W. Weller, U. S. Bureau of Mines Report of Inv. 5571 (1960).
- ¹⁸E. N. Fomichev, N. P. Slyusar, A. D. Krivorotenko, and V. Ya. Tolstaya, *Ogneupory* **7**, 36 (1973).
- ¹⁹*Thermochemical Data for Reactor Materials and Fission Products*, edited by E. H. P. Corfundke and R. J. M. Konings (Elsevier, Amsterdam, 1989).
- ²⁰K. Nagarajan, R. Saha, R. Babu, and C. K. Mathews, *Thermochim. Acta* **90**, 297 (1985).
- ²¹R. C. Liebermann, L. E. A. Jones, and A. E. Ringwood, *Phys. Earth Planet Inter.* **14**, 165 (1977).
- ²²K. Itoh, K. Ochiai, H. Kawaguchi, C. Moriyoshi, and E. Nakamura, *Ferroelectrics* **159**, 85 (1994).
- ²³S. Devanarayanan and P. S. Narayanan, *Indian J. Pure Appl. Phys.* **6**, 714 (1968).
- ²⁴D. L. Branson, *J. Am. Ceram. Soc.* **48**, 441 (1965).
- ²⁵Y. Zhao and D. J. Weidner, *Phys. Chem. Minerals* **18**, 294 (1991).
- ²⁶M. D. Mathews, E. B. Mirza, and A. C. Momin, *J. Mater. Sci. Lett.* **10**, 305 (1991).
- ²⁷E. Takayama-Muromachi and A. Navrotsky, *J. Solid State Chem.* **72**, 244 (1988).
- ²⁸I. Hatta, Y. Shiroishi, K. A. Müller, and W. Berlinger, *Phys. Rev. B* **16**, 1138 (1977).
- ²⁹J. A. M. van Roosmalen, P. van Vlaanderen, and E. H. P. Cordfunke, *J. Solid State Chem.* **101**, 59 (1992).
- ³⁰N. Ohama, H. Sakashita, and A. Okazaki, *Phase Transitions* **4**, 81 (1984).
- ³¹M. Sato, Y. Soejima, N. Ohama, A. Okazaki, H. J. Scheel, and K. A. Müller, *Phase Transitions* **5**, 207 (1985).
- ³²M. O'Keefe, B. G. Hyde, and J. O. Bovin, *Phys. Chem. Minerals* **4**, 299 (1979).
- ³³K. A. Müller, Y. Luspain, J. L. Servoin, and F. Gervais, *J. Phys. (Paris) Lett.* **43**, L537 (1982).
- ³⁴M. D. Fontana, G. Métrat, J. L. Servoin, and F. Gervais, *J. Phys. C* **16**, 483 (1984).
- ³⁵B. Gautason and K. Muhlenbachs, *Science* **260**, 518 (1993).
- ³⁶J. P. Coughlin and E. G. King, *J. Am. Chem. Soc.* **72**, 2262 (1950).
- ³⁷X. Liu and R. C. Liebermann, *Phys. Chem. Minerals* **20**, 171 (1993).
- ³⁸H. D. Megaw, *Mater. Res. Bull.* **6**, 1007 (1971).
- ³⁹X. Liu, Y. Wang, R. C. Liebermann, P. D. Maniar, and A. Navrotsky, *Phys. Chem. Minerals* **18**, 224 (1991).
- ⁴⁰Y. Zhao, D. J. Weidner, L. Topor, and A. Navrotsky, *Trans. Am. Geophys. Union* **72**, 478 (1991).
- ⁴¹Y. Zhao, D. J. Weidner, J. B. Parise, and D. E. Cox, *Phys. Earth Planet Inter.* **76**, 1 (1993).